CERN-FASER-CONF-2023-002
30 August 2023

Observation of high-energy electron neutrino interactions with FASER's emulsion detector at the LHC

FASER Collaboration

This note presents the first results from the search for high-energy electron and muon neutrino charged-current interactions in the FASERν emulsion/tungsten sub-detector of FASER. A subset of the FASERν volume is used, corresponding to a target mass of 68 kg, exposed to 9.5 fb^{-1} of LHC proton-proton collision data with a centre-of-mass energy of 13.6 TeV. Following stringent selections requiring a lepton (electron or muon) with reconstructed energy above 200 GeV, three electron neutrino interactions are observed with an expected background of 0.002 ± 0.003, leading to a statistical significance of the neutrino signal of 5 standard deviations. This is the first direct observation of electron neutrino interactions at a particle collider, and the signal events include neutrinos with $\sim$ TeV energies, the highest-energy electron neutrinos detected from an artificial source. Four muon neutrino interactions are also found, with an expected background of 0.5 ± 0.3, leading to a statistical significance of the muon neutrino signal of 2.5 standard deviations.

CONTENTS

I. INTRODUCTION

One of the primary physics goals of the FASER experiment [1–3] at CERN's Large Hadron Collider (LHC) [4] is to study high-energy neutrinos produced in the LHC collisions using the dedicated FASERν sub-detector [5, 6]. FASERν is a tungsten/emulsion detector placed in front of the main FASER detector [7]. The emulsion allows extremely precise reconstruction of charged particle tracks originating from neutrino interactions inside the tungsten, and it can be used to identify and measure the energy of muon tracks and electromagnetic showers from electrons, enabling the identification of both the electron and muon charged-current (CC) neutrino interactions.[1]

Neutrinos are copiously produced via hadron decay in the LHC collisions, forming a collimated beam around the beam collision axis line of sight (LOS). Neutrinos close to the LOS are produced with very high energy and therefore have relatively large interaction cross section, with energies up to several TeV. Since they are weakly interacting, the neutrinos are not affected by the natural FASER shielding of the 100 m of rock and magnetic fields traversed between the collision point and the detector, which reduces backgrounds significantly.

In this note the first observation of neutrino interactions in FASERν is reported. Only a small fraction of the total FASERν volume is analysed, corresponding to a target mass of 68 kg. The direct detection of the first neutrino interaction candidates at the LHC using the 2018 pilot detector was reported in 2021 [8]. The first observation of muon neutrinos produced at a collider using the electronic FASER detector components was released in March 2023 [9], and more recently the SND@LHC Collaboration [10, 11] has also reported the observation of muon neutrino interactions at the LHC [12].

The main background to neutrino detection at FASER arises from neutral hadrons interacting in the detector. The neutral hadrons generally have lower energy than the neutrinos, and they are therefore suppressed using appropriate selections on topological and kinematic variables related to the reconstructed interaction vertex. Further requirements of a high-energy electron or muon signature provide an additional background suppression and allow to distinguish ν_μ and ν_e CC interactions.

The current analysis is the first step of a broad physics programme of neutrino measurements at the LHC, which will provide important insights in neutrino and electroweak physics, as well as QCD via probing forward hadron production and deep inelastic scattering of high-energy neutrinos in the target, as detailed in Refs. [13, 14].

II. THE FASERν DETECTOR

The FASERν detector is made up of 730 layers of interleaved tungsten plates and emulsion films, with a total target mass of 1.1 tonnes. The tungsten plates are 1.1 mm thick and each emulsion film is 0.34 mm thick. The detector is 1 m long and 25×30 cm^2 in the plane transverse[2] to the incoming neutrino beam. The detector is placed in front of the main FASER detector and is aligned with the beam collision axis LOS, 480 m away from the collision point inside the ATLAS experiment (IP1). FASERν is described in more detail in Refs. [6, 7].

For the first FASERν analysis presented in this note, only a small fraction of the detector volume is used. Fig. 1 shows the analysed volume. In the transverse (x-y) plane, a region of 24 cm $\times$ 9 cm is analysed, and 16.5 cm in the longitudinal direction (150 tungsten plates), corresponding to a

[1] In this note charge conjugation is implied such that $\nu_{\mu/e}$ represents the sum of both $\nu_{\mu/e}$ and $\overline{\nu}_{\mu/e}$.

[2] A cartesian coordinate system is used with the z-axis running along the LOS from the ATLAS collision point to FASER, the y-axis pointing vertically upwards, and the x-axis pointing horizontally to the centre of the LHC ring. The angle ϕ is the azimuthal angle in the x-y plane, and θ is the polar angle measured from the positive z-axis.

target mass of 68 kg. The data from an additional 100 plates, immediately downstream of the target region, are used in the analysis to follow down tracks and measure their momentum. The LOS passes through close to the centre of the analysed volume in the horizontal plane and about 2 cm from the bottom of the analysed area in the vertical plane.

The emulsion films are read out by the Hyper Track Selector (HTS) system [15]. The HTS system divides each emulsion film into eight readout zones. The first alignment between every two consecutive films is performed for each readout zone using recorded track hits. The data is then divided into sub-volumes of 1.7 cm × 1.7 cm × 15 films. After the second alignment between every two consecutive films and track reconstruction in each sub-volume, an additional alignment is applied by selecting tracks crossing 15 plates to improve the tracking resolution. Finally, the track reconstruction procedure links track hits on different films by correlating their positions and angles. The track reconstruction algorithm is based on that of the NA65/DsTau experiment and is described in Ref. [16]. The reconstructed data quality was checked using penetrating muons. Fig. 2 shows the measured position resolution of 0.28 μm in a plane transverse to the beam. The track hit efficiency in each film was measured to be greater than 90% in the reconstructed volumes, corresponding to an efficiency of 99.98% for detecting tracks with at least three hits out of seven films.

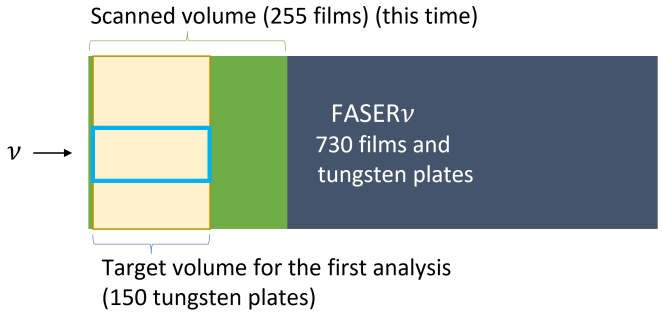

FIG. 1. Schematic view of the analysed volume.

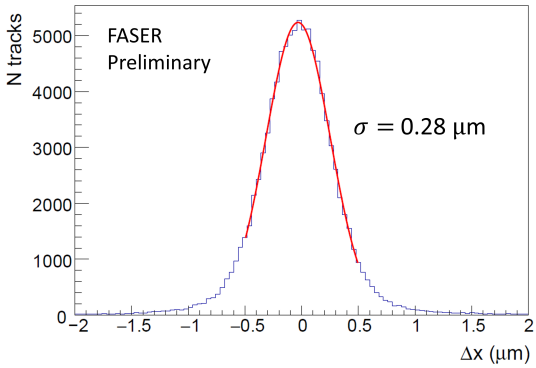

FIG. 2. Distribution of the position deviation between the track hits and the straight-line fitting to reconstructed tracks, measured in the analysed volume. The red line shows the fit of a Gaussian distribution to the data to extract the resolution, with a fitted resolution of 0.28 μm.

III. THE DATA AND SIMULATION SAMPLES

The analysed dataset was collected between July 26th and September 13th 2022, in which the LHC delivered 9.5 fb^{-1} of proton–proton collision data with a centre-of-mass energy of 13.6 TeV to IP1. The luminosity measurement is provided by the ATLAS experiment [17–19]. The charged particle flux within 10 mrad of the angular peak, which is dominated by energetic muons, is 1.29×10^4 tracks/cm^2/fb^{-1} normalized by luminosity.

Monte Carlo (MC) simulation samples for neutrino and background processes are used to define the selection requirements and to estimate the backgrounds and uncertainties. The interaction of neutrinos with the tungsten/emulsion detector is simulated using the GENIE event generator [20, 21]. The neutrino energy spectra and relative flavour composition are based on Ref. [22]. All interactions of particles traversing the FASER detector are simulated using GEANT4 [23].

To estimate the expected number of neutrino events, several of the assumptions of Ref. [22] are adjusted: the center-of-mass energy, beam crossing angle, and LOS alignment are corrected, and the average of the neutrino flux from the predicted light and heavy hadron production of `DPMJET` [24, 25] and `SIBYLL` [26] are used with the uncertainty spanning their full difference. The expected number of neutrino interactions in the analysed region before any selections is 29.4 ± 5.0 for ν_μ and 11.8 ± 7.5 for ν_e.

The main background in this analysis arises from neutral hadrons produced in photo-nuclear interactions in the rock in front of FASER or in the FASERν detector material, initiated by high-energy muons produced at IP1. There is a flux of around 0.5 Hz/cm^2 of high-energy muons passing through FASER during nominal LHC running. The neutral-hadron background is simulated via a multi-step simulation process. First, the energy spectra of the muons is simulated using FLUKA [27, 28], which includes a detailed model of the LHC infrastructure between IP1 and FASER. Then, GEANT4 is used to simulate muons interacting in the rock in front of FASER or in the tungsten of the FASERν detector with the energy spectra predicted by the FLUKA simulations. Finally, high-statistics samples of the individual neutral-hadron species (neutral kaons, neutrons and lambdas) are produced and weighted to follow the energy spectra estimated by the previous step.

IV. VERTEX SELECTION

Candidate CC neutrino interactions are selected based on reconstructed charged particle tracks, forming a neutral vertex in the emulsion.

Fig. 3 shows the MC simulation energy spectrum of neutral hadrons emerging from rock or produced within the detector, compared to the spectrum of neutrinos interacting in the detector. The number of neutral hadrons drops quickly with increasing energy. Since neutrinos are more energetic than the neutral-hadron background, the tracks associated to the vertex are required to be boosted in the forward direction. The CC interaction signature produces a high-energy lepton (electron or muon), which is well separated in azimuthal angle from the other particles associated to the vertex.

A. Initial vertex selection

Using reconstructed tracks passing through at least three plates, vertex reconstruction is performed by searching for converging patterns of tracks with a minimum distance within 5 μm. Tracks

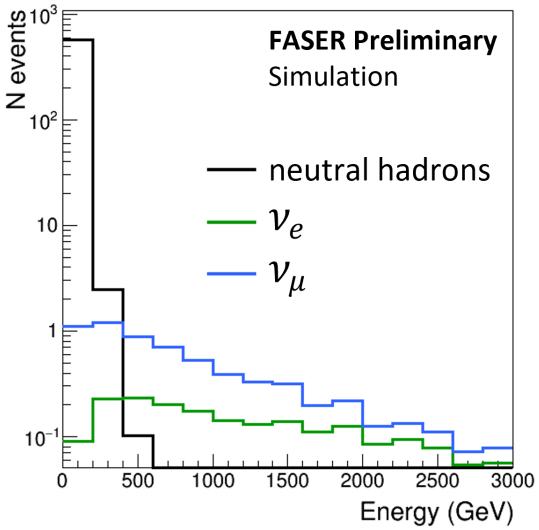

FIG. 3. MC simulation distributions of the energy of neutral hadrons produced by muon interactions (black), as well as neutrinos interacting with the detector: ν_e (green) and ν_μ (blue). The distributions correspond to 2 fb^{-1}.

with $\tan\theta \leq 0.5$ are used. Converging patterns with more than four tracks are selected as vertices. An additional selection was applied to these vertices to suppress neutral hadrons: the number of tracks with $\tan\theta \leq 0.1$ relative to the beam direction is required to be greater than three.

The vertices are categorized as charged (where the vertex is from the interaction of a charged particle) or neutral (where the vertex is from the interaction of a neutral particle, as in the case of neutrinos) based on the presence or absence, respectively, of charged parent tracks. A charged parent track is a track with at least three track hits detected within ten films upstream of the reconstructed vertex with an impact parameter to the vertex within 5 μm and with a minimum distance to at least three vertex tracks within 3 μm. A looser set of selections in the track reconstruction procedure is used for finding the charged parent track, with a track reconstruction inefficiency of less than 10^{-5}. The background from charged vertices being selected as signal vertices is thus negligible.

B. Electron identification and energy measurement

Candidate electron neutrino CC interaction vertices are selected from the initial set of vertices by requiring an associated high-energy electromagnetic (EM) shower with reconstructed energy above 200 GeV. The high-energy EM shower is then required to have the azimuthal angle relative to the sum of all other tracks in the vertex, $\Delta\phi > \pi/2$. The EM shower is formed from reconstructed segments in the emulsion produced by electron/positron pair production as the shower develops. Given the short radiation length of tungsten the associated EM shower is compact, and can be well associated with the vertex.

Fig. 4 shows the concept of the EM shower reconstruction. It is based on a cylinder around the shower axis, and the energy measurement uses the number of segments in ± 3 films around the shower maximum (seven films in total) in the longitudinal direction. The segments used are required to be connected to more than two films and to satisfy selections on the angle from the shower axis ($\delta\theta < 10$ mrad) and the distance (position displacement from the shower axis δpos $<$

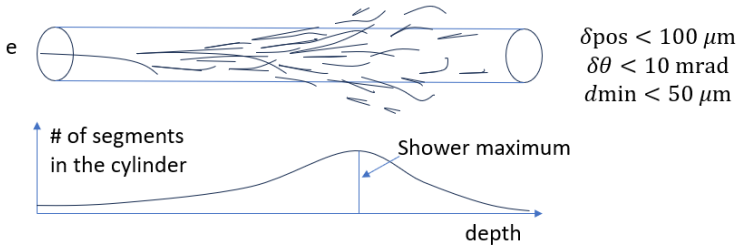

FIG. 4. Schematic view of the definition for the cylinder with 100 μm radius, catching the electromagnetic shower from the primary electron generated in ν_e CC interactions.

100 μm, minimum distance between the shower axis line and track line upstream of the segment $d\text{min} < 50$ μm) to reduce the effect of background segments. Additionally, the average background is estimated by using random cylinders and then subtracted from the shower before the energy estimate. The energy reconstruction algorithm performance is tested in MC simulation (Fig. 5). It shows a resolution of around 25% for EM energies at 200 GeV and between 25-40% at higher energies, depending on the electron angle. In the future, the EM energy reconstruction performance will be further calibrated following a testbeam in 2023 using high-energy electrons at the CERN SPS.

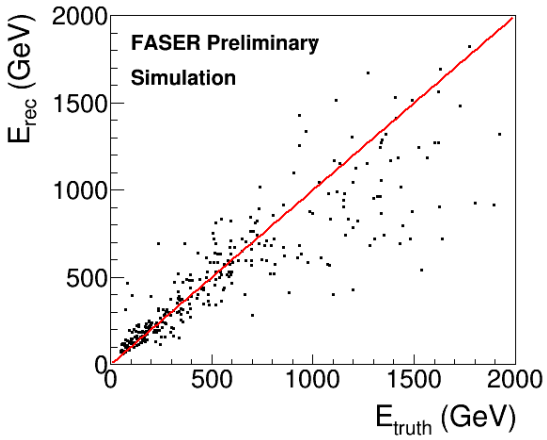

FIG. 5. The reconstructed electron energy versus the true energy in ν_e CC MC simulation.

C. Muon identification and momentum measurement

Candidate muon neutrino CC interaction vertices are selected from the initial set of vertices by requiring that one of the reconstructed charged particle tracks associated with the vertex penetrates more than 100 tungsten plates without exhibiting secondary hadron interactions and have a reconstructed momentum greater than 200 GeV. Simulation studies show that the probability for a charged hadron with $p > 200$ GeV to satisfy this requirement is about 60%. The high-momentum long track is then required to have the azimuthal angle relative to the sum of all other tracks associated to the vertex, $\Delta\phi > \pi/2$.

The track momentum is estimated by measuring Multiple Coulomb Scattering using the so-called coordinate method [29]. The performance of the momentum estimate is studied using simulation,

including smearing to account for residual mis-alignments between the emulsion films, and shows a resolution of around 20% at 200 GeV (Fig. 6) and between 20–30% at higher energies. The track momentum estimation performance is validated in data, by studying the momentum of long tracks by splitting these into two tracks, and comparing the reconstructed momentum of the two halves.

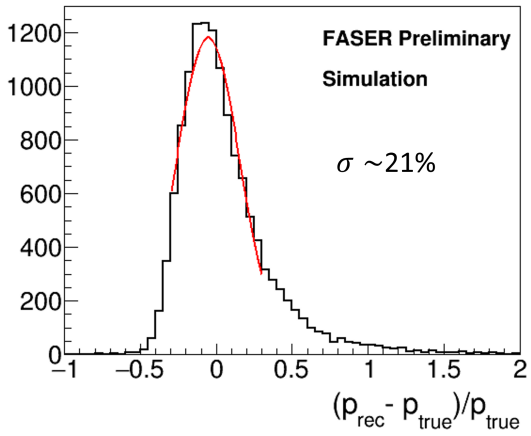

FIG. 6. The resolution of the muon momentum measurement for muons with momentum in the range 100–300 GeV in MC simulation. The red line shows the fit of a Gaussian distribution to the simulated data to extract the resolution, with a fitted resolution of 21%.

V. BACKGROUNDS

The background from neutral-hadron interactions is estimated from the MC simulation samples detailed in Section III. The final samples used are normalized to the equivalent luminosity of the data, by using the number of muons observed in the data and simulations to derive the scaling factor. The final neutral-hadron samples are equivalent to 15 to 20 times the size of the data.

The modelling of the neutral-hadron background in the simulation is validated in data using the initial neutral-vertex sample (before the high-energy lepton selection is applied), which is dominated by neutral-hadron interactions. The expected number of hadron interaction vertices is 216, and the number of vertices in the data is 140 (7 of which satisfy the high-energy CC interaction selection requirements). Fig. 7 shows a comparison of the number of tracks in the vertex, and the reconstructed momentum of the highest momentum track between the neutral-hadron MC and the data, where the MC distributions are normalized to data to aid comparison. The shapes of the distributions are well modelled in the simulation, and the number of interactions is compatible at better than the 50% level, with more neutral-hadron interactions predicted in the MC than observed in the data.

Table I shows the selected number of neutral-hadron events in the simulation when applying both the ν_μ and ν_e selections, and also with reduced lepton energy requirements of 50 GeV. The samples studied were K_S, K_L, n, $\overline{n}$, Λ and $\overline{\Lambda}$, but only those in which at least one event passed any of the selections are included in the table.

The background estimate for the ν_μ CC selection is taken directly from the MC simulation as 0.32 ± 0.15 vertices, if accounting only for the statistical uncertainty. A 50% systematic uncertainty is assigned related to the modelling of the neutral-hadron interactions in the MC.

Since no neutral-hadron MC event passes the full ν_e selection, the background is estimated from the number of selected events with the looser requirement on the electron energy of 50 GeV.

Simulation studies show that for lepton energy requirements above 50 GeV, the dependence of the number of selected neutral-hadron events as a function of the lepton energy requirement is similar when evaluated with either the muon or electron neutrino selections. The background to the electron selection is therefore estimated as:

$$\mathrm{N(had)}_{\nu_e}^{200\ \mathrm{GeV}} = \mathrm{N(had)}_{\nu_e}^{50\ \mathrm{GeV}} \times \frac{\mathrm{N(had)}_{\nu_\mu}^{200\ \mathrm{GeV}}}{\mathrm{N(had)}_{\nu_\mu}^{50\ \mathrm{GeV}}}, \tag{1}$$

where $\mathrm{N(had)}_{\mathrm{A}}^{\mathrm{B\ GeV}}$, is the number of neutral-hadron events passing the selection A, with the lepton energy requirement of B GeV. This leads to a final estimate of $\mathrm{N(had)}_{\nu_e}^{200\ \mathrm{GeV}} = 0.002 \pm 0.002$ vertices, where the statistical uncertainty is shown. A systematic uncertainty of 100% is assigned to cover both the modelling of the neutral-hadron interactions in the MC, as well as the uncertainties related to the scaling of the estimate to the higher electron energy requirement.

TABLE I. Number of events satisfying the different selections for neutral-hadron MC simulation samples. Both the raw number of MC events passing the selections, and the number scaled to the analysis dataset are shown.

Selection	Quantity	K_L	n	Λ	Total
ν_μ selection $E > 50$ GeV	Raw MC events	77	71	70	-
ν_μ selection $E > 200$ GeV	Raw MC events	1	3	2	-
	Scaled to analysis dataset	0.07	0.16	0.10	0.32
ν_e selection $E > 50$ GeV	Raw MC events	0	1	0	-
ν_e selection $E > 200$ GeV	Raw MC events	0	0	0	-
	Scaled to analysis dataset	0	0	0	0

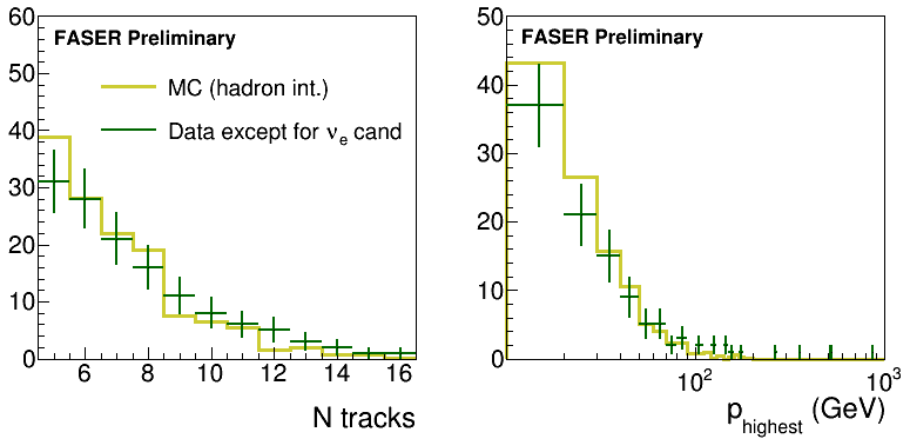

FIG. 7. MC simulation distributions of track multiplicity and momentum of the highest momentum track from vertices of the hadronic interactions. The observed events in the data sample, except for ν_e candidate events, are shown in green. The MC simulation distributions are normalized to the number of observed tracks.

In addition to the neutral-hadron background, there is a contribution to the vertices selected by the muon CC selection from neutral-current (NC) neutrino interactions. This is estimated by

using MC simulation as 0.19 ± 0.15 vertices, where the uncertainty includes the contribution from the incoming neutrino flux.

The number of expected vertices from background sources, including neutral-hadron interactions and NC neutrino interactions, is shown in Table II for both the ν_μ and ν_e selections.

TABLE II. The number of expected vertices from background sources including neutral-hadron interactions and NC neutrino interactions after the ν_μ and ν_e selections.

Background	ν_μ CC	ν_e CC
Neutral-hadron interactions	0.32 ± 0.15 (stat.) ± 0.16 (syst.)	0.002 ± 0.002 (stat.) ± 0.002 (syst.)
NC neutrino interactions	0.19 ± 0.15	-
Total	0.51 ± 0.27	0.002 ± 0.003

VI. RESULTS

Three vertices are selected by the ν_e selection in data. The properties of the selected vertices are compared with the expectation from ν_e CC simulation in Fig. 8. Four vertices are selected with the ν_μ selection in data. The properties of these selected vertices are compared with the expectation from ν_μ CC simulation in Fig. 9 and for the properties related to the individual tracks forming the vertex in Fig. 10. In general the simulation describes the data well for these variables. The position of the selected vertices in the transverse plane are shown in Fig. 11. Event displays of an example selected ν_e candidate vertex and a ν_μ candidate vertex are shown in Fig. 12.

The selected electron neutrino interaction candidates have reconstructed electron energies of 1.5 TeV, 700 GeV, and 400 GeV. These are therefore the highest-energy ν_e interactions detected by accelerator-based experiments.

The expected number of neutrino signal events satisfying the selections are in the ranges 0.6–5.2 (for ν_e CC) and 3.0–8.6 for (for ν_μ CC), where the range covers the predictions of the different event generators, but does not include the systematic uncertainty related to the vertex selection. The observed number of interactions is compatible with the expectation.

The statistical significance of the observation of the ν_e and ν_μ candidate events is estimated by considering the confidence for excluding the null (background-only) hypothesis. The probability to obtain the observed number of ν_e and ν_μ candidate events from the background is estimated by generating 5000 toy events based on a Poisson Probability Density Function (PDF) whose mean is the sum of all background contributions. The backgrounds from the various neutral-hadron components (K_L, neutron, Λ) are generated following a separate Poisson distribution for each species. For ν_μ this is based on the expected background satisfying the nominal momentum requirement, while for ν_e it is based on the number of events satisfying the lower energy requirement described above multiplied by the scaling factor to the nominal energy requirement. On top of this, a Gaussian-distributed systematic uncertainty of 50% (100%) in the ν_μ (ν_e) case is included. Finally, the NC neutrino background is generated following a Gaussian PDF, centred on the MC expectation and with a width equal to its total uncertainty. Based on the combined PDF, an observed p-value of 1.60×10^{-7} for ν_e (5.17×10^{-3} for ν_μ) is obtained, corresponding to a significance of 5σ for ν_e (2.5σ for ν_μ) for the exclusion of the null hypothesis.

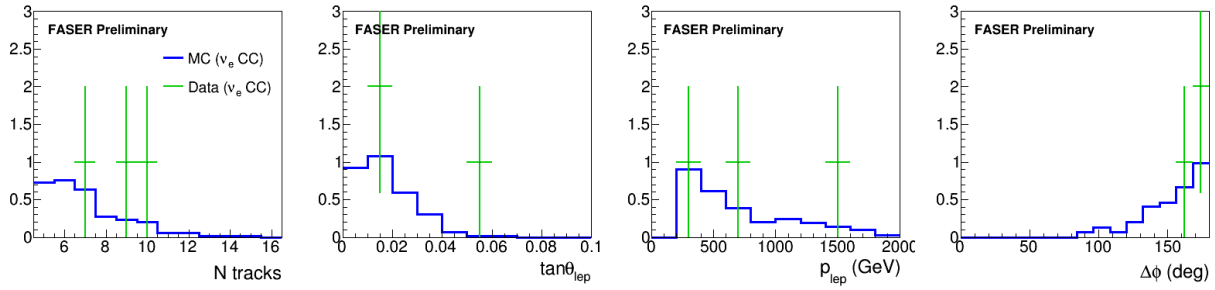

FIG. 8. MC simulation distributions of the track multiplicity, electron angle, electron energy, and $\Delta\phi$ for the ν_e CC signal. The observed ν_e CC candidate events in the data sample are shown in green. The MC simulation distributions are normalized to the number of observed events.

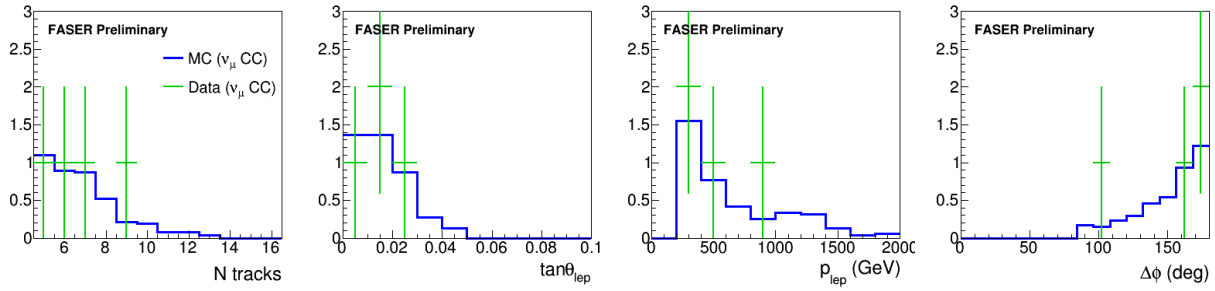

FIG. 9. MC simulation distributions of the track multiplicity, muon angle, muon momentum, and $\Delta\phi$ for the ν_μ CC signal. The observed ν_μ CC candidate events in the data sample are shown in green. The MC simulation distributions are normalized to the number of observed events.

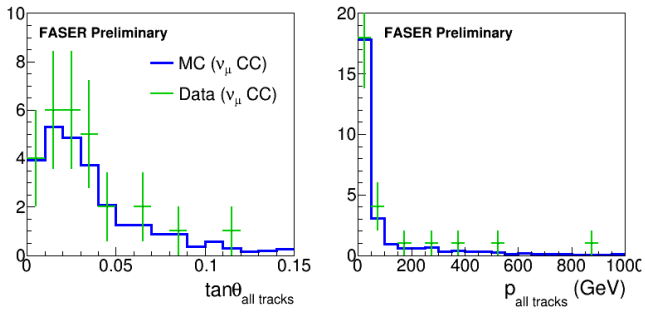

FIG. 10. MC simulation distributions of track angle and momentum from vertices of the ν_μ CC signal. The observed ν_μ CC candidate events in the data sample are shown in green. The MC simulation distributions are normalized to the number of observed tracks.

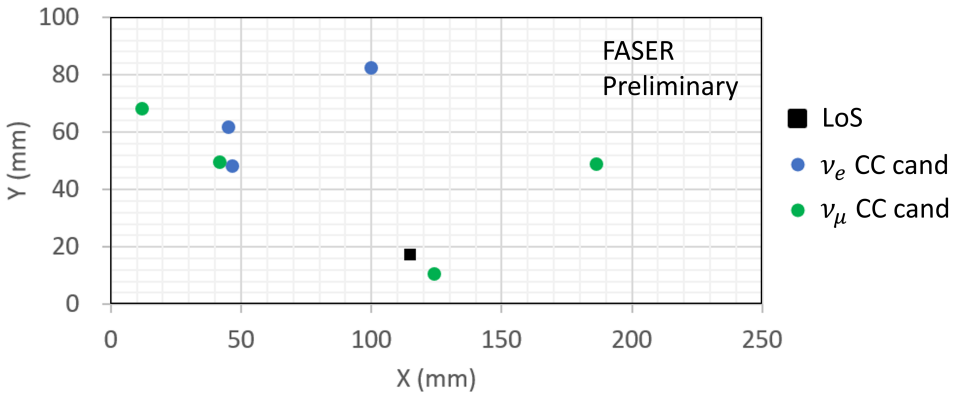

FIG. 11. Vertex positions in the transverse plane of the observed ν_e CC and ν_μ CC candidate events in the data sample. The uncertainty on the vertex position is less than 10 μm, whereas the uncertainty in the LOS position is about 1 cm.

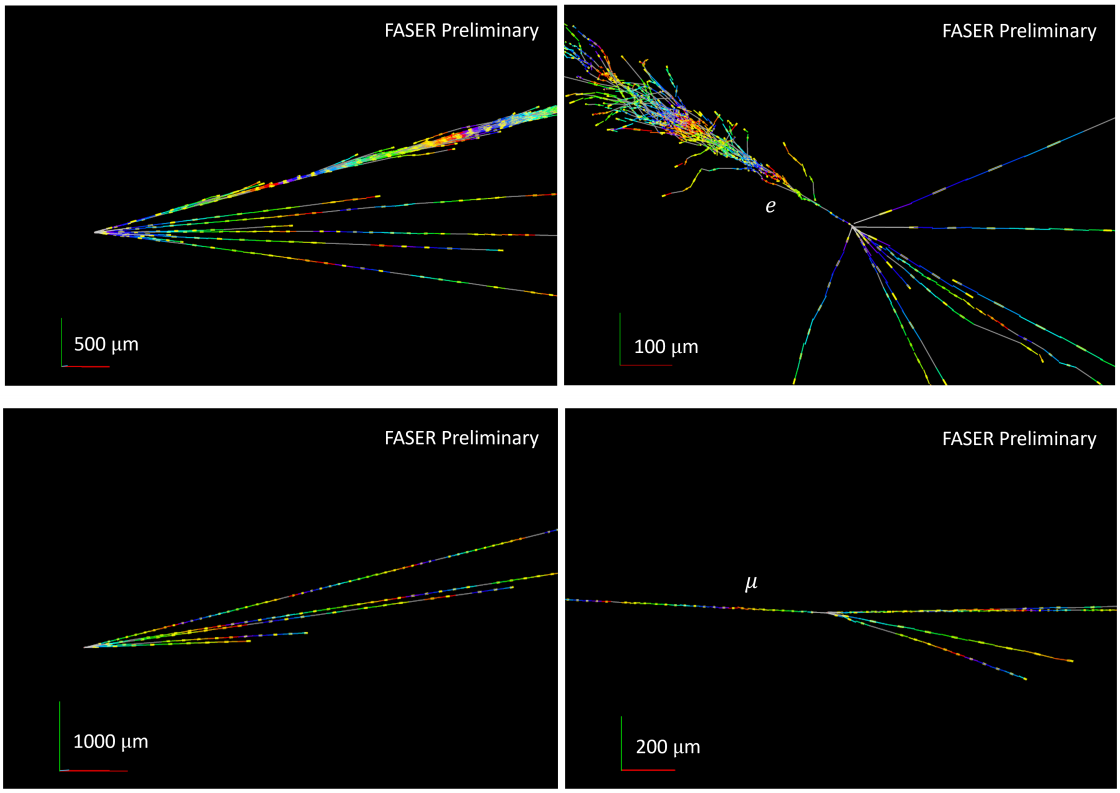

FIG. 12. Event displays of one of the ν_e CC candidate events (top) and one of the ν_μ CC candidate events (bottom). The right panels show the views transverse to the beam direction.

VII. CONCLUSIONS

First results for the search for high-energy electron and muon neutrino interactions in the FASERν tungsten/emulsion detector have been presented. The analysis uses a subset of the FASERν volume, corresponding to a target mass of 68 kg, exposed to 9.5 fb^{-1} of LHC proton collision data in the summer of 2022. Selections are applied to retain reconstructed vertices consistent with high-energy CC electron and muon neutrino interactions, while minimizing the background from neutral-hadron interactions. Three electron neutrino candidate vertices are selected with an expected background of 0.002 ± 0.003, leading to a statistical significance of the neutrino signal of 5 standard deviations. This represents the first direct observation of electron neutrinos produced at a particle collider. Four muon neutrino candidate vertices are selected with an expected background of 0.5 ± 0.3, leading to a statistical significance of the neutrino signal of 2.5 standard deviations. These results demonstrate the ability to carry out neutrino studies with the FASERν emulsion-based detector at the LHC.

VIII. APPENDIX

Fig. 13 shows additional event displays of selected neutrino interaction vertices.

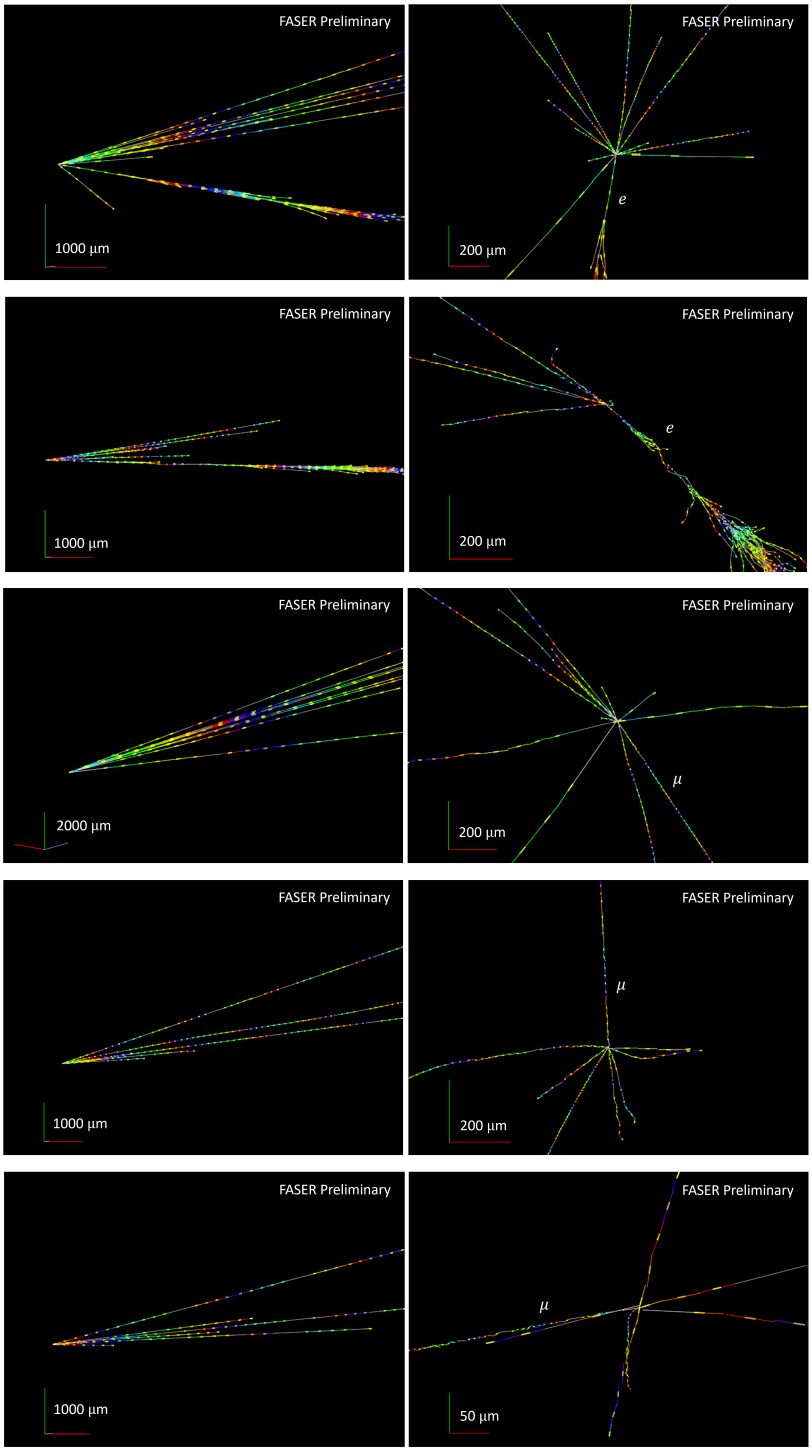

FIG. 13. Event displays of ν_e and ν_μ CC candidate events. The right panels show the views transverse to the beam direction.

[1] J. L. Feng, I. Galon, F. Kling, and S. Trojanowski, "ForwArd Search ExpeRiment at the LHC," *Phys. Rev. D* **97** (2018) no. 3, 035001, arXiv:1708.09389 [hep-ph].

[2] **FASER** Collaboration, A. Ariga *et al.*, "Letter of Intent for FASER: ForwArd Search ExpeRiment at the LHC," arXiv:1811.10243 [physics.ins-det].

[3] **FASER** Collaboration, A. Ariga *et al.*, "Technical Proposal for FASER: ForwArd Search ExpeRiment at the LHC," arXiv:1812.09139 [physics.ins-det].

[4] L. Evans and P. Bryant, "LHC Machine," *JINST* **3** (2008) S08001.

[5] **FASER** Collaboration, H. Abreu *et al.*, "Detecting and Studying High-Energy Collider Neutrinos with FASER at the LHC," *Eur. Phys. J. C* **80** (2020) no. 1, 61, arXiv:1908.02310 [hep-ex].

[6] **FASER** Collaboration, H. Abreu *et al.*, "Technical Proposal: FASERnu," arXiv:2001.03073 [physics.ins-det].

[7] **FASER** Collaboration, H. Abreu *et al.*, "The FASER Detector," arXiv:2207.11427 [physics.ins-det].

[8] **FASER** Collaboration, "First neutrino interaction candidates at the LHC," *Phys. Rev. D* **104** (2021) no. 9, L091101, arXiv:2105.06197 [hep-ex].

[9] **FASER** Collaboration, H. Abreu *et al.*, "First Direct Observation of Collider Neutrinos with FASER at the LHC," *Phys. Rev. Lett.* **131** (2023) no. 3, 031801, arXiv:2303.14185 [hep-ex].

[10] **SHiP** Collaboration, C. Ahdida *et al.*, "SND@LHC," arXiv:2002.08722 [physics.ins-det].

[11] **SND@LHC** Collaboration, G. Acampora *et al.*, "SND@LHC: The Scattering and Neutrino Detector at the LHC," arXiv:2210.02784 [hep-ex].

[12] **SND@LHC** Collaboration, R. Albanese *et al.*, "Observation of Collider Muon Neutrinos with the SND@LHC Experiment," *Phys. Rev. Lett.* **131** (2023) no. 3, 031802, arXiv:2305.09383 [hep-ex].

[13] L. A. Anchordoqui *et al.*, "The Forward Physics Facility: Sites, experiments, and physics potential," *Phys. Rept.* **968** (2022) 1–50, arXiv:2109.10905 [hep-ph].

[14] J. L. Feng *et al.*, "The Forward Physics Facility at the High-Luminosity LHC," *J. Phys. G* **50** (2023) no. 3, 030501, arXiv:2203.05090 [hep-ex].

[15] M. Yoshimoto, T. Nakano, R. Komatani, and H. Kawahara, "Hyper-track selector nuclear emulsion readout system aimed at scanning an area of one thousand square meters," *PTEP* **2017** (2017) no. 10, 103H01, arXiv:1704.06814 [physics.ins-det].

[16] **DsTau** Collaboration, S. Aoki *et al.*, "DsTau: Study of tau neutrino production with 400 GeV protons from the CERN-SPS," *JHEP* **01** (2020) 033, arXiv:1906.03487 [hep-ex].

[17] ATLAS Collaboration, "Luminosity determination in pp collisions at $\sqrt{s} = 13$ TeV using the ATLAS detector at the LHC," arXiv:2212.09379 [hep-ex].

[18] G. Avoni *et al.*, "The new LUCID-2 detector for luminosity measurement and monitoring in ATLAS," *JINST* **13** (2018) no. 07, P07017.

[19] ATLAS Collaboration, "Preliminary analysis of the luminosity calibration of the ATLAS 13.6 TeV data recorded in 2022." ATL-DAPR-PUB-2023-001, 2023. https://cds.cern.ch/record/2853525.

[20] C. Andreopoulos *et al.*, "The GENIE Neutrino Monte Carlo Generator," *Nucl. Instrum. Meth. A* **614** (2010) 87–104, arXiv:0905.2517 [hep-ph].

[21] C. Andreopoulos, C. Barry, S. Dytman, H. Gallagher, T. Golan, R. Hatcher, G. Perdue, and J. Yarba, "The GENIE Neutrino Monte Carlo Generator: Physics and User Manual," arXiv:1510.05494 [hep-ph].

[22] F. Kling and L. J. Nevay, "Forward neutrino fluxes at the LHC," *Phys. Rev. D* **104** (2021) no. 11, 113008, arXiv:2105.08270 [hep-ph].

[23] **GEANT4** Collaboration, S. Agostinelli *et al.*, "GEANT4: A Simulation toolkit," *Nucl. Instrum. Meth.* **A506** (2003) 250–303.

[24] S. Roesler, R. Engel, and J. Ranft, "The Monte Carlo event generator DPMJET-III," in *International Conference on Advanced Monte Carlo for Radiation Physics, Particle Transport Simulation and Applications (MC 2000)*, pp. 1033–1038. 12, 2000. arXiv:hep-ph/0012252.

[25] A. Fedynitch, *Cascade equations and hadronic interactions at very high energies*. PhD thesis, KIT, Karlsruhe, Dept. Phys., 11, 2015.

[26] F. Riehn, R. Engel, A. Fedynitch, T. K. Gaisser, and T. Stanev, "Hadronic interaction model Sibyll 2.3d and extensive air showers," *Phys. Rev. D* **102** (2020) no. 6, 063002, arXiv:1912.03300 [hep-ph].

[27] A. Ferrari *et al.*, "FLUKA: A multi-particle transport code (Program version 2005),".

[28] G. Battistoni *et al.*, "Overview of the fluka code," *Annals of Nuclear Energy* **82** (2015) 10–18. Joint International Conference on Supercomputing in Nuclear Applications and Monte Carlo 2013, SNA + MC 2013. Pluri- and Trans-disciplinarity, Towards New Modeling and Numerical Simulation Paradigms.

[29] K. Kodama, N. Saoulidou, G. Tzanakos, B. Baller, B. Lundberg, R. Rameika, J. Song, C. Yoon, S. Chung, S. Aoki, T. Hara, C. Erickson, K. Heller, R. Schwienhorst, J. Sielaff, J. Trammell, K. Hoshino, J. Kawada, M. Komatsu, M. Miyanishi, M. Nakamura, T. Nakano, K. Narita, K. Niwa, N. Nonaka, K. Okada, O. Sato, T. Toshito, S. Miyamoto, S. Takahashi, B. Park, T. Furukawa, V. Paolone, and T. Kafka, "Momentum measurement of secondary particle by multiple coulomb scattering with emulsion cloud chamber in donut experiment," *Nuclear Instruments and Methods in Physics Research Section A: Accelerators, Spectrometers, Detectors and Associated Equipment* **574** (2007) no. 1, 192–198. https://www.sciencedirect.com/science/article/pii/S0168900207002677.